



Kinetics of phyllosemiquinone oxidation in the Photosystem I reaction centre of *Acaryochloris marina*

Stefano Santabarbara^{a,b,*}, Benjamin Bailleul^{a,1}, Kevin Redding^c, James Barber^d,
Fabrice Rappaport^a, Alison Telfer^d

^a *Institute de Biologie Physico-Chimique, UMR 7141 CNRS-UPMC, 13 rue P. et M. Curie, 75005 Paris, France*

^b *Istituto di Biofisica, Consiglio Nazionale delle Ricerche, Via Celoria 26, 20133 Milano, Italy*

^c *Department of Chemistry and Biochemistry, Arizona State University, S. Rural Road, Tempe, AZ 85287-1604, USA*

^d *Division of Molecular Biosciences, Imperial College London, Biochemistry Building, South Kensington Campus, London SW7 2AZ, UK*

ARTICLE INFO

Article history:

Received 8 August 2011

Received in revised form 10 October 2011

Accepted 11 October 2011

Available online 19 October 2011

Keywords:

Bidirectional electron transfer

Photosystem I

Chlorophyll *d*

Radical pair

Phylloquinone

Acaryochloris marina

ABSTRACT

Light-induced electron transfer reactions in the chlorophyll *a/d*-binding Photosystem I reaction centre of *Acaryochloris marina* were investigated in whole cells by pump-probe optical spectroscopy with a temporal resolution of ~5 ns at room temperature. It is shown that phyllosemiquinone, the secondary electron transfer acceptor anion, is oxidised with bi-phasic kinetics characterised by lifetimes of 88 ± 6 ns and 345 ± 10 ns. These lifetimes, particularly the former, are significantly slower than those reported for chlorophyll *a*-binding Photosystem I, which typically range in the 5–30 ns and 200–300 ns intervals. The possible mechanism of electron transfer reactions in the chlorophyll *a/d*-binding Photosystem I and the slower oxidation kinetics of the secondary acceptors are discussed.

© 2011 Elsevier B.V. All rights reserved.

1. Introduction

Chlorophyll (Chl) *d* is the most abundant chromophore bound to the photosynthetic pigment protein complexes of the cyanobacterium *Acaryochloris marina* [1–3]. Typically the Chl *d* to Chl *a* ratio exceeds 10, although the exact stoichiometry is dependent on the irradiance conditions during growth [4,5]. Chl *d* absorption, in vivo is about 30–35 nm red-shifted with respect to that of Chl *a* henceforth extending the possibility of performing oxygen evolution by the absorption of near-infrared photons (e.g. [1–6]). In addition, α -carotene is found in *A. marina* in place of β -carotene.

The Photosystem I (PS I) reaction centre of *A. marina* binds more than 90 Chl *d* molecules and 1 to 2 molecules of Chl *a* [3,7–9]. Although the majority of the Chl *d* molecules bound to PS I in *A. marina* have light harvesting function [3,6], it has been shown both by optical [7,10–12]

and electron paramagnetic resonance [8,13,14] spectroscopies that the stable cation species generated following photochemical charge separation resides on a Chl *d*, or, possibly, a Chl *d*–Chl *d'* hetero-dimer [5,8]. Based on the maximum of the differential absorption bleaching in the Q_y transition, this chemical species is referred to as $P_{740}^{(+)}$ [7,8,10,11]. The redox midpoint potential of the P_{740}/P_{740}^+ couple was originally reported to be up-shifted by 85–155 mV with respect to stable donor cation of Chl *a*-binding PS I reaction centres [7]. However, recent re-investigations yielded values of $E_{P_{740}^+/P_{740}}^0$ ranging from 425 to 450 mV [9,11,12], which are in the same range as the values reported for the P_{700}^+/P_{700} redox couple (reviews in Ref. [15]). As the energy input is about 100 meV smaller in Chl *d* as compared to Chl *a* containing PS I, the conserved free energy level of the cation suggests that the reducing power produced by charge separation may be lower in *A. marina* as discussed in refs. [9,11,12].

At present, the mechanism of primary charge separation in PS I of *A. marina* is not fully elucidated. Ultra-fast optical transient spectroscopy suggests that Chl *a* might be involved in electron transfer reactions in *A. marina* [8,10], either as an electron acceptor, equivalent to A_0 in Chl *a*-binding PS I, or as the primary electron donor, equivalent to the accessory Chls in PS I (see [16]). The subsequent electron acceptor, which is commonly known as A_1 has been shown to be, as in the case of Chl *a*-binding PS I reaction centres (RC), a phylloquinone (PhQ) molecule [8,9,14]. The kinetics of oxidation of A_1^- in *A.*

Abbreviations: Chl, chlorophyll; DCMU, 3–3,4 dichlorophenyl-1,1-dimethylurea; FCCP, carbonyl-cyanide-*p*-trifluoromethoxy-phenylhydrazone; PhQ, phylloquinone; PS (I/II), Photosystem (I/II); RC, reaction centres; $P^{(+)}$ or P_{700}^+/P_{740}^+ , PS I electron donor (cation)

* Corresponding author at: IBF/CNR, Via Celoria 26, 20133 Milano, Italy. Tel.: +39 02 50314857; fax: +39 02 503 4815.

E-mail address: stefano.santabarbara@cnr.it (S. Santabarbara).

¹ Present address: Benjamin Bailleul, Institute of Marine and Coastal Sciences, Rutgers, The State University of New Jersey, 71 Dudley Road, New Brunswick, NJ 08901-8525, USA.

marina, as estimated by the pulsed-EPR technique at 265 K [14], appear to be slightly slower (~450 ns) with respect to the slow phase of A_1^- oxidation in Chl *a*-binding PS I complexes (~300 ns) (e.g. [15,17]). The fast component of A_1^- oxidation, which is ~20 ns at room temperature [15,17], is generally not observable by electron paramagnetic spectroscopy. On the other hand, the kinetics of charge recombination measured at 77 K yield a value of 150 μ s, which falls within the range determined for Chl *a*-binding PS I reaction centres [11]. Moreover, the functional distance between the spin densities of P_{740}^+ and A_1^- of 25.23 ± 0.05 Å [14] is essentially the same as that determined for Chl *a*-binding PS I (reviewed in Ref. [18]). Hence, the structural organisation of the electron transfer chain in PS I appears to be conserved, in PS I reaction centres whether they bind mainly Chl *d* or Chl *a*. This idea is further confirmed by the large degree of homology of the genes *psaA* and *psaB* coding for the reaction centre subunits of *A. marina* with respect to other oxygenic phototrophic organisms [19], even though they are the least homologous amongst different cyanobacterial strains. Similar homology is also observed for the *psaC* gene, which codes for the subunit binding the terminal electron acceptors, iron-sulphur clusters F_A and F_B . EPR [8,14] and optical spectroscopy [7,11] indicate that the characteristics of F_A and F_B in *A. marina* are virtually unaltered with respect to these cofactors when bound to the Chl *a*-binding RCs. Indeed, it was noticed that all PS I subunits of *A. marina* display high homology with respect to other cyanobacterial strains, except for the *PsaI* and *PsaX* genes [19].

Even though a clear picture of the structural and chemical nature of the electron transfer cofactors bound to the PS I reaction centre of *A. marina* is emerging, there is a lack of clear understanding of the dynamics of electron transfer reactions. In particular, secondary electron transfer involving phylloquinone A_1 and successive electron acceptors has only been investigated in frozen samples (265 K and 77 K, [14]). The value reported for a close-to-physiological temperature, was determined in time-resolved EPR experiments, which, in general, suffer from relatively limited time-resolution (~50 ns). Furthermore the lifetime determined by such techniques might be biased by magnetic relaxation processes which, together with the electron transfer reaction rates, contribute to the decay of the electron spin echo signal (for a discussion see Ref. [20]).

In order to characterise the oxidation kinetics of A_1^- in the PS I reaction centre of *A. marina* at room temperature further we have investigated electron transfer reactions in living cells of this organism using optical pump-probe spectroscopy having a temporal resolution of ~5 ns. Results are compared with those obtained in a Chl *a*-binding cyanobacterial model system, *Synechocystis sp.* PCC 6803. It is shown that the kinetics of A_1^- oxidation are bi-phasic, characterised by slower lifetimes than are seen in Chl *a* PS I, 88 ± 6 ns and 345 ± 10 ns compared to 18 ± 4 and 285 ± 10 , respectively. Possible models of secondary electron transfer in the Chl *d*-binding PS I RC are discussed.

2. Material and methods

Cultures of *A. marina* were grown under continuous illumination ($15 \mu\text{E m}^{-2} \text{s}^{-1}$) in K + ESM medium [21], except that the $\text{FeSO}_4 \cdot 7\text{-H}_2\text{O}$ level was increased to 4 mg L^{-1} . The cells were shaken vigorously to allow sufficient aeration. Cultures of *Synechocystis sp.* PCC 6803 were grown in BG11 medium, under continuous illumination and aerated by air bubbling. The cultures were harvested during semi-logarithmic growth by centrifugation at 5500 g for 5 min, and immediately suspended in the growth medium supplemented with 20% W/V Ficoll to avoid sedimentation during the measurements. 3-(3,4 dichlorophenyl)-1,1-dimethylurea (DCMU) ($20 \mu\text{M}$) and hydroxylamine (1 mM) were added to the cell suspension to suppress PS II photochemistry and carbonyl-cyanide-*p*-trifluoromethoxyphenylhydrazine (FCCP) ($8 \mu\text{M}$) was used to dissipate transmembrane ionic gradients.

2.1. Optical spectroscopy

Light-induced optical transients were monitored with a home-built pump-probe spectrometer which has been previously described in detail [22]. In brief, the actinic flash is provided by a dye laser (LDS 698) pumped by a frequency double Nd-YAG laser (Quantel, Brilliant). The excitation wavelength was 700 nm, the bandwidth of the actinic pulse is ~7 ns and the intensity is adjusted to excite ~70% of the reaction centres. The transients are probed by the out-put of an Optical Parametric Oscillator (OPO), pumped by a frequency tripled Nd-YAG laser (Continuum, Surelite). For measurements in the near-UV the output of the OPO is frequency doubled. The pump-probe delay is controlled by a home-built pulse programmer. The excitation (pump) flashes were fired with a frequency of 0.2 Hz, which allows for the cellular electron transfer chain to return to the dark-adapted condition between each flash. The kinetic traces are acquired firstly by scanning the pump-probe sequence from short to long delays followed by a reverse (long to short) series and each pump-probe point is sampled twice. Typically, four to eight of these sequences were averaged depending of the signal-to-noise at a given wavelength. The increased averaging, and hence the increased experimental time, is generally required in the near UV.

2.2. Data analysis

Optical transients acquired at multiple wavelengths were fitted to a sum of exponential functions by a global minimisation routine as previously described [23,24].

3. Results

Laser flash-induced transient absorption kinetics, were recorded in living cells of *A. marina* (Fig. 1) and *Synechocystis sp.* PCC 6803 (Fig. 2) and monitored through the near-UV and the visible spectrum. The kinetic traces were fitted by a sum of exponential functions using a global fitting routine. In *A. marina* a satisfying agreement is obtained by considering three decay components characterised by lifetimes of 88 ± 4 ns, 345 ± 10 ns and $11 \pm 0.7 \mu\text{s}$, as shown in Fig. 1 for selected wavelengths. In *Synechocystis sp.* PCC 6803 the best fit yields lifetimes of 18 ± 4 ns, 285 ± 10 ns and $7.5 \pm 0.5 \mu\text{s}$, also shown at selected wavelengths in Fig. 2. Moreover, in both organisms, a non-decaying component (within the experimental time window of 10 ns–20 μs) needs to be considered. Extending the time window to 1 ms, it was determined that this signal decays with a lifetime of $125 \pm 25 \mu\text{s}$ in *A. marina* cells, and $140 \pm 15 \mu\text{s}$ in *Synechocystis sp.* PCC 6803 cells (Fig. 3). The decay associated spectra (DAS) resulting from the global fit of the kinetics in the 10 ns–20 μs interval are presented in Fig. 4.

3.1. Long-living and microsecond decay components

The spectra associated with the non-decaying component (up to 20 μs) recorded in vivo are consistent with difference spectra arising from oxidation of the meta-stable electron donor, P_{740} , of *A. marina* and P_{700} in *Synechocystis*. The reduction lifetime of $125 \pm 25 \mu\text{s}$ derived from an experiment performed on an extended time scale is also consistent with the reduction of the meta-stable oxidised electron donor occurring through a diffusion-limited process involving a soluble electron donor, which in the case of *A. marina* is probably plastocyanin ([12], but see also Ref. [25] for discussion of electron donors).

Diffusion controlled rates of P^+ reduction are most commonly observed in prokaryotes (reviewed in Ref. [26]). In agreement with this, the rate of P_{700}^+ reduction in *Synechocystis* is determined as $140 \pm 15 \mu\text{s}$. The DAS associated with the non decaying component (in the 10 ns–20 μs time window, Fig. 4D) obtained in *Synechocystis sp.* PCC 6803 suggests that the electron donor, under the growth

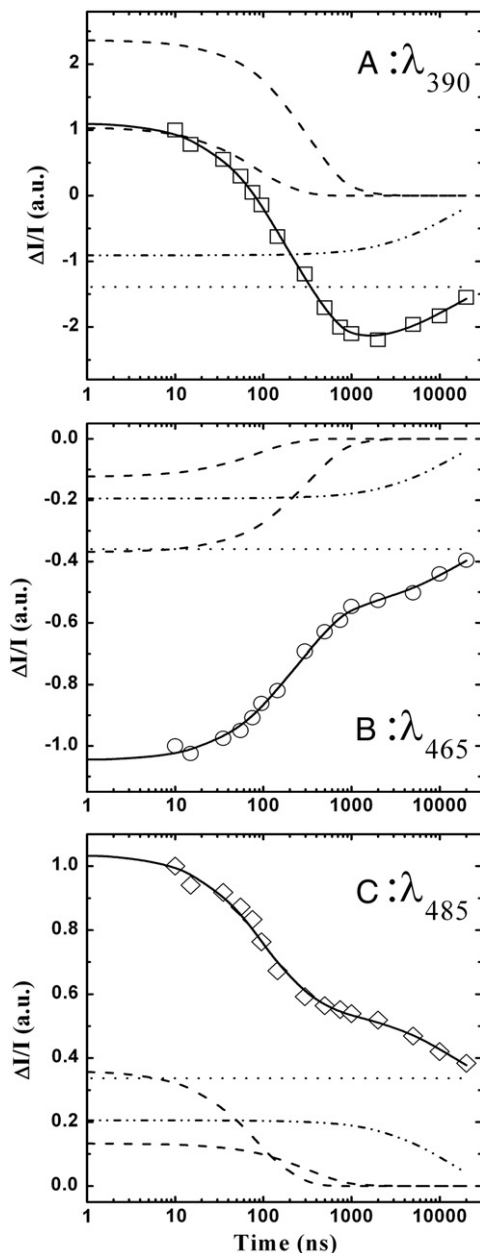


Fig. 1. Laser-flash induced absorption difference kinetics recorded in whole cells of *A. marina* monitored at 390 nm (A, open squares), 465 nm (B, open circles) and 485 nm (C, open diamonds). Also presented at each wavelength are the best fits in terms of linear combination of exponential functions (solid lines) as well as the contribution of each decay components: dashed lines (sub-microsecond, 88 ns and 345 ns), dash-dotted lines: 11 μ s; dotted lines: non-decaying. Each decay trace is normalised on the initial amplitude at 10 ns delay from the actinic flash.

conditions employed in this study, is also plastocyanin since, as in the case of *A. marina* (Fig. 4C), there is no evidence for cytochrome *c* marker bands in the 400–425 nm region.

The relatively slow rate of P_{740}^+ reduction, suggests that either a binary complex, comprised of PSI and plastocyanin (PSI:PC), is not formed in the dark or, if so, only in a small fraction of centres. This is in contrast to what is most commonly observed in eukaryotes [23,26,27]. This observation, based on kinetic studies (Figs. 1–3), is also supported by sequence alignment of the *PsaF* gene, which shows that two lysine residues known to be important for formation of the PSI:electron-donor complex (e.g. [27]), allowing fast reduction of P^+ , are not conserved in *A. marina*.

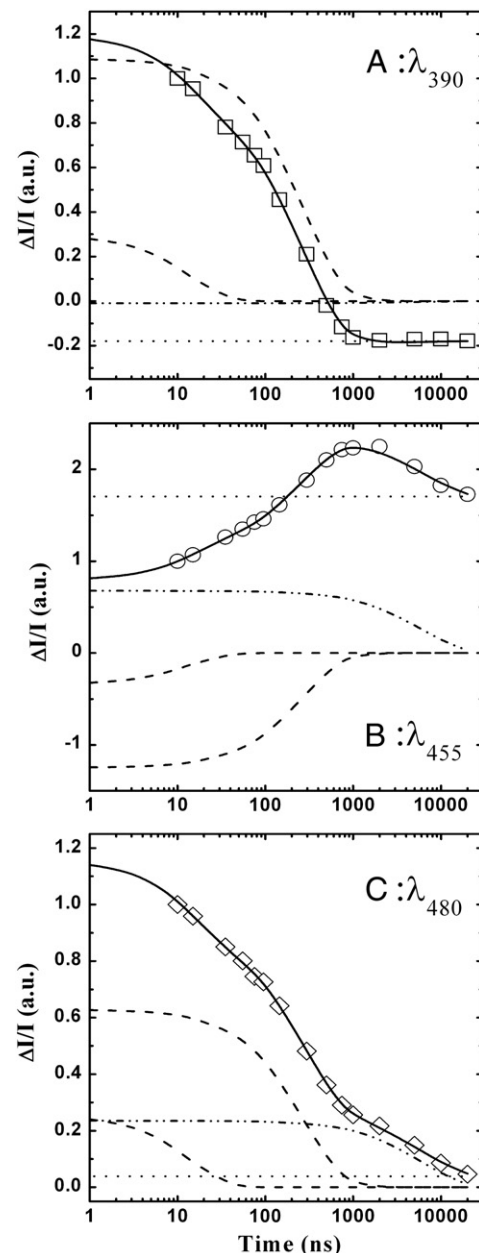


Fig. 2. Laser-flash induced absorption difference kinetics recorded in whole cells of *Synechocystis sp.* PCC 6803 monitored at 390 nm (A, open squares), 455 nm (B, open circles) and 480 nm (C, open diamonds). Also presented at each wavelength are the best fits in terms of linear combination of exponential functions (solid lines) as well as the contribution of each decay components: dashed lines (sub-microsecond, 14 ns and 285 ns), dash-dotted lines: 7 μ s; dotted lines: non-decaying. Each decay trace is normalised on the initial amplitude at 10 ns delay from the actinic flash.

In *A. marina* the spectrum associated with the non-decaying transient absorption change is consistent with the $[P_{740}^+ - P_{740}]$ spectrum previously presented for isolated PS I reaction centres [7,11]. It displays maximal bleaching at 455 nm, and a shoulder at 435 nm. In *Synechocystis sp.* PCC 6803 this DAS is dominated by the bleaching of the meta-stable electron donor P_{700}^+ , which is a Chl *a*/Chl *a'* heterodimer. It displays maximal bleaching at 432 nm and a shoulder located at 418 nm. The comparison of these spectra, obtained in whole cells, provide further confirmation that, in PS I of *A. marina*, the electron hole is localised on Chl *d* as previously proposed based on studies using purified complexes [7–11,13,14]. Other differences in the DAS of the non-decaying components recorded in the Chl *a*-binding RC of *Synechocystis* and Chl *d*-binding RC of *A. marina* cells are also

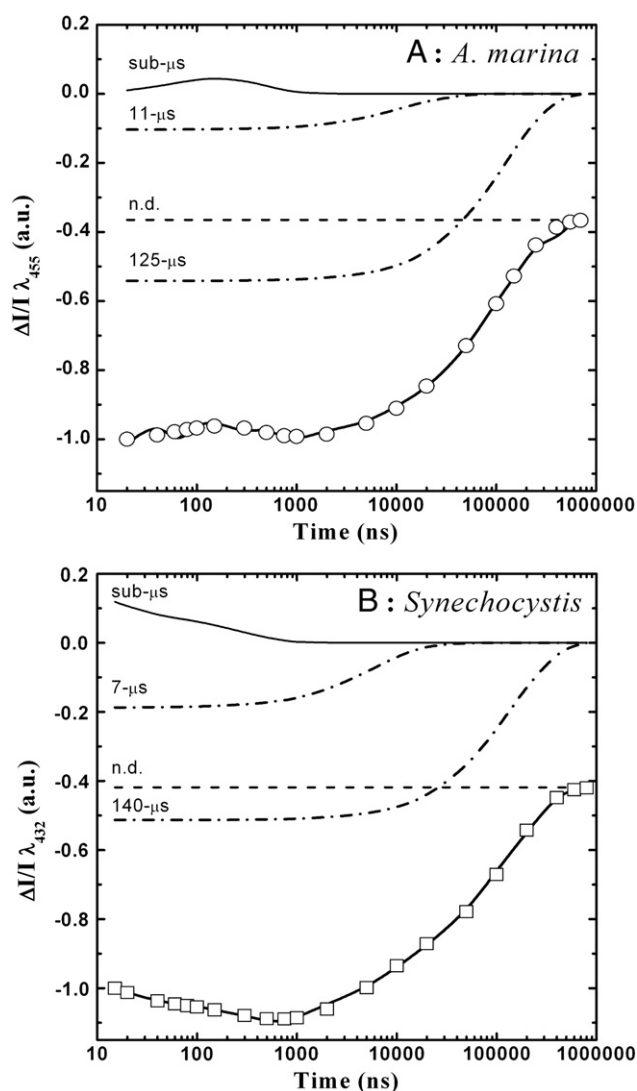


Fig. 3. Laser-flash induced absorption difference kinetics on an extended time-scale (10 ns–700 μ s) recorded in whole cells of *A. marina* (A) and *Synechocystis* sp. PCC 6803 (B), at the wavelength of maximal differential bleaching, 455 nm and 432 nm, respectively. Open symbols: experimental data; thick solid lines: fits in terms of linear combination of exponential functions. Also shown are the contribution of each decay component: thin solid lines (sum of sub-microsecond components, see Figs. 1 and 2 for details), dash-dotted lines: μ s components (values are indicated in the figures); dashed lines: non-decaying. The traces are normalised on the initial amplitude.

observed. A sharp positive feature is observed in *A. marina* at 475 nm together with a broader band peaking at \sim 515 nm. In *Synechocystis* sp. PCC 6803 the maxima of the positive features peak at 450 nm and 498 nm, i.e. \sim 20–25 nm blue-shifted (compare panels C and D of Fig. 4). These features are likely to result from local electrochromic band-shifts due to the positive charge sitting on P^+ , which is sensed by Chl *a* and β -carotene, in the case of *Synechocystis* [28], and Chl *d* and α -carotene, in the case of *A. marina*.

The DAS of the components falling in the μ s time-window (Fig. 4) are also different in the two organisms. In *Synechocystis*, the 7- μ s phase has a spectrum which resembles the non-decaying DAS. Therefore, we assigned it to a population (\sim 15–20%) of reaction centres in which P_{700}^+ is reduced rapidly, probably as a result of a preformed complex between PS I and the reduced electron carrier in the dark (see also Ref. [29]). In *A. marina* the DAS of the 11- μ s phase, also displays a small amplitude throughout the spectral window investigated, as observed in *Synechocystis*. However, the 11- μ s DAS is markedly different from that of the non-decaying component. It shows bleaching at

400 nm, 445 nm and 460 nm and a broad positive feature peaking at \sim 520 nm. The spectrum and the lifetime are consistent with the relaxation of a carotene triplet, probably α -carotene which is the most abundant carotenoid in *A. marina* and the only one detected in purified PS I complexes [9]. This species is likely to be populated by energy transfer from a Chl *d* excited state, which was shown to be populated with comparable yield to that of Chl *a* (i.e. \sim 60% in organic solutions) [30,31], formed either in the DCMU-inhibited PS II core complexes or its associated antenna.

3.2. Nanosecond decay components

Even though the decay in the sub-microsecond timescale is described by biphasic kinetics both in *Synechocystis* sp. PCC 6803 (18 and 285 ns) and in *A. marina* (88 and 345 ns), significant differences in the value of the decay lifetimes are observed. Generally, the recovery kinetics of light-induced absorption differences are slower in *A. marina* compared to those of *Synechocystis*. However, whereas the value of the longest of sub- μ s decay is only about 20% slower in *Acar-yochloris* (345 ± 10 ns) compared to *Synechocystis* (285 ± 10 ns), a fourfold difference is observed for the faster component (88 ± 6 and 18 ± 4 ns in *A. marina* and *Synechocystis*, respectively).

The lifetimes and the DAS associated with the 20-ns and 280-ns components retrieved from the global analysis of the flash-photolysis experiment in *Synechocystis* cells (Fig. 4B) are in extremely good agreement with those previously presented for PS I particles isolated from the same organism (e.g. [28,29,32]). These are assigned to the reoxidation of the PsaB- and PsaA-bound phyllosemiquinones, A_{1B} and A_{1A} , respectively. The most characteristic spectral features are absorption in the near-UV (330–400 nm range), which reflect primarily the PhQ⁻-PhQ absorption difference, and bands in the 470–520 nm region arising mostly from electrochromic band-shifts of Chl *a* and β -carotene, in response to the electric field associated with the radical pair [$P_{740}^+A_1^-$]. The relative amplitude between the fast and slow phyllosemiquinone oxidation phases is 0.25:0.75 (averaged in the near-UV), as commonly observed in Chl *a*-binding RCs of cyanobacteria [28,29,32].

In *A. marina* the DAS of the 88-ns and 345-ns components also display broad absorption bands in the near-ultraviolet. For both components the maximal differential absorption is observed at 385 nm; a shoulder at 365 nm is clearly resolved only in the DAS of the 345-ns component, consistent with differential absorption changes arising from the oxidation of phyllo(semi)quinone, which has been proposed to act as the secondary electron acceptor in this RC as well [8,14]. The relative amplitude between the 88-ns and the 345-ns phases, averaged between 370 and 405 nm, is $0.32 \pm 0.05:0.67 \pm 0.05$, which shows a somewhat larger contribution of the faster decay phase with respect to that observed in the Chl *a*-binding RC of *Synechocystis*. Moreover, we note that the DAS of both the 88-ns and 345-ns components in the near-UV appear to be slightly blue-shifted compared to those of the 18-ns and 285-ns components observed in cells of *Synechocystis* sp. PCC 6803 (panels A and B of Fig. 4), as well as those previously recorded in other Chl *a*-binding PS I reaction centres (e.g. reviewed in Refs. [28,29,32]). For instance, in the 285-ns component of Chl *a*-binding RCs, the main features in the near UV, peak at \sim 375, 401 and 435 nm, whereas in the 345-ns component of Chl *d*-binding RC they are shifted to 364, 389 and 426 nm.

The DAS of the 88-ns and 345-ns components also differ markedly in the blue region. A strong derivative-shaped spectral feature is observed in the DAS of the 345-ns DAS, having a maximum at 448 nm and a minimum at 465 nm, but this is not seen in the 88-ns DAS. Spectral structures similar to those observed in the 345-ns component of *A. marina* are seen in the Chl *a*-binding RC (Fig. 4 and see [28]), albeit blue shifted by 10–15 nm. They have been assigned to electrochromic band-shifts of Chl chromophores [31]; the red-shift of the peak positions in *A. marina* suggests that in this organism the

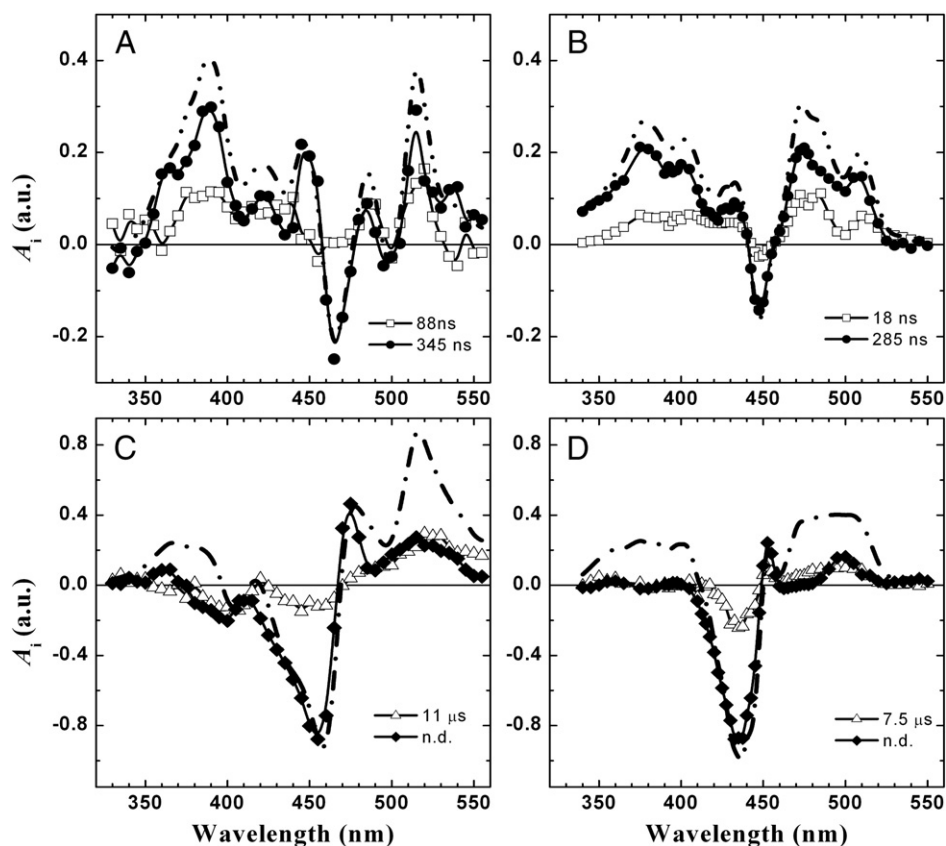


Fig. 4. Decay associated spectra (DAS) derived from global analysis of laser flash-photolysis kinetics in whole cells of *A. marina* (A, C) and *Synechocystis* sp. PCC 6803 (B, D). Panel A (*A. marina*) and B (*Synechocystis*) show the DAS of the sub-microsecond decay phases. Squares: “fast” ns-component; circles: “slow” nanosecond component; dash-dotted line is the sum of the two phases. Panel C (*A. marina*) and D (*Synechocystis*) show the DAS of the long living components; triangles: microsecond component; diamonds: non-decaying component (in 10 ns–20 μ s window), the dash dotted lines shows the “initial” spectra extrapolated to $t \rightarrow 0$.

electric field-sensitive chromophore is probably Chl *d*. Notably, the intensity of the 448 nm–465 nm derivative-shaped feature observed in the 88-ns DAS in *A. marina* is significantly less pronounced than the 18-ns component of *Synechocystis* sp. PCC 6803 PS I. Spectral features arising from the electrochromic effect on α -carotene are observed in both the 88-ns and the 345-ns DAS. In both cases peaks are observed at 480–485 nm and 515 nm, and bleaching is observed at 485–500 nm. The 345-ns DAS also displays a positive signal at 540 nm which is absent in the 88-ns DAS.

The spectral features observed in the 345-ns component, including the blue shift of the near-UV absorption with respect to Chl *a*-binding RC and the presence of a derivative-like structure centred at \sim 450 nm, were previously reported by Schenderlein et al. [11], who investigated the recombination reaction between P_{740}^+ and A_1^- in isolated reaction centres at 77 K. This observation further confirms our assignment of the 345-ns component to A_1^- oxidation. The characteristic difference in the visible region of the spectrum between the 88-ns and 345-ns DAS suggests that these two lifetimes of 88 ns and 345 ns are associated with two distinct electron transfer reactions. At the same time, the 88-ns DAS also shows significant differential absorption in the near-UV (Fig. 4), indicating that, as with the 345-ns component, it is also likely to reflect a reaction involving the oxidation of a semiquinone species.

4. Discussion

Using whole cells we have found that oxidation of the secondary electron acceptor A_1^- in the Chl *d*-binding PS I RC of *A. marina*, displays bi-phasic kinetics (Fig. 1), which are characterised by time constants of 88 ± 6 ns and 345 ± 10 ns. Non-monotonic kinetics of A_1^-

oxidation have been commonly reported for the case of the more extensively studied Chl *a*-binding PS I reaction centres (see Refs. [15,17,33] for reviews). Here, we have confirmed this by reinvestigation of PS I electron transfer reactions in whole cells of *Synechocystis* sp. PCC 6803 (Fig. 2), to allow direct comparison under identical conditions.

In Chl *a*-binding PS I complexes, the best characterised phases of A_1^- oxidation have lifetimes in the 5–30 ns and 200–300 ns ranges [15,17,33]. A so-called intermediate component in the 160–180 ns interval, assigned to inter Fe–S electron transfer reactions, was observed in site-directed mutants of the A_{1A} binding site that slowed electron transfer from A_{1A} sufficiently to resolve them kinetically [34,35]. It is generally accepted that in Chl *a*-binding PS I both the PsaA- and PsaB-bound cofactors participate in electron transfer reactions (e.g. [36,37]) and that the fast (\sim 20 ns) and slow (\sim 250 ns) oxidation phases reflect, principally, reactions involving the phyllosemiquinones, A_{1B}^- and A_{1A}^- , respectively [15,17,34–36].

Moreover, in the Chl *a* PS I RC, the DAS associated with the 20-ns and 250-ns lifetimes display characteristic signatures that make them distinct both in the near-UV, where the differential absorption is dominated by the $[\text{PhQ}^- \text{F}_X - \text{PhQF}_X^-]$ spectrum, as well as in the wavelength region above 470 nm, where the differential absorption reflects local electrochromic effects, principally on β -carotenes, but also on Chl *a* [28]. As is apparent from the data shown in Fig. 4, for data recorded in *Synechocystis* cells, the 250-ns DAS shows a structured spectrum in the near-UV, whereas that of the 20-ns DAS is relatively featureless. Similarly, a pronounced derivative like feature with a maximum at 420 nm and minimum at 450 nm is observed in the 250-ns DAS, whereas it is less pronounced in the 20-ns DAS. Moreover, it has been possible to ascribe the differences in the

electrochromic band-shift region of the DAS to the effect on different carotene molecules, which sense preferentially electron transfer involving either A_{1A} or A_{1B} [28].

Similar to what is commonly reported for Chl *a*-binding PS I-RC, the DAS of the 88-ns and 345-ns components detected in *A. marina* shows characteristic differences, i.e. the 345-ns DAS has a more structured spectrum in the near-UV and a marked derivative feature centred at ~455 nm, which is essentially absent in the 88-ns spectrum. Thus, some of the most obvious differences seen between the DAS of the faster and slower components in *A. marina* are part of a general phenomenon previously observed in PS I from other species. The biphasic kinetics and the differences in the DAS point towards the occurrence of bi-directional electron transfer in the RC of this organism. If this is the case, the relative amplitude of the fast and slow ns phases could be taken as a first-order indication of the relative utilisation of the two parallel electron transfer branches. In the Chl *d*-binding RC of *A. marina*, we observed fractional amplitudes, on average, of ~0.3:0.7, which represents a slightly higher relative contribution of the “faster” (88-ns) phase compared to Chl *a*-binding RC of *Synechocystis sp.* PCC 6803 ~0.25:0.75 (Fig. 4). On the other hand, fractional amplitudes similar to the ratio observed in *A. marina* are commonly observed in other Chl *a*-binding RCs, such as those of green algae (e.g. [7,15,23,35–38]).

Another indication of bidirectional electron transfer in *A. marina* comes from the previously reported heterogeneity of electron transfer at cryogenic temperature [11,14], where the acceptors F_A/F_B were only stably reduced in a fraction of centres, whereas charge recombination between P_{740}^+ and A_1^- was observed in the remainder. Heterogeneity of electron transfer at low temperatures is also a characteristic feature of Chl *a* binding PS I-RC [33,37–40], which has been interpreted qualitatively in the frame of a bidirectional electron transfer model, in which irreversible $F_{A/B}$ reduction takes place on the B-branch below ~100K, whereas charge recombination occurs on the A-branch (e.g. [20,37,38,40]).

However, it is important to mention that biphasic semiquinone oxidation, by itself, does not constitute proof for the functionality of two electron transfer chains. Before there was firm evidence for this, which required independent genetic manipulation of the two branches (e.g. [15,17,24,34–38,42–45]), the biphasic oxidation of A_1^- was explained in the framework of a mono-directional electron transfer model invoking a low driving force for this particular reaction [33,39]. At the same time heterogeneous electron transfer at cryogenic temperature was explained in terms of a distribution of the standard redox potentials of the acceptor and donor molecules, so that the reaction would be thermodynamically favourable in a fraction of reaction centres and unfavourable in others [33,49]. It is important to recall this issue, because Itoh and co-workers [8,41] noted that there exists an asymmetry in the primary sequences of the PsaA and PsaB subunits in *A. marina*, which might lead to unidirectional electron transfer. While the Met residue that coordinates Chl *ec-A3* (A_0) is conserved in the PsaA subunit of *A. marina*, a Leu is found in the PsaB sequence. This observation, together with a stoichiometry of less than 2 Chl *a* per PS I, indicating an apparent deficiency of Chl *a* in one of the branches, led to the proposal that electron transfer reactions in the PS I reaction centres of *A. marina* involve a single functional branch [8,41]. However, both the reported stoichiometry and the involvement of Chl *a* in electron transfer reactions in PS I of *A. marina* remain matters of controversy [8,41].

Moreover, amino-acid substitution of the methionine acting as an axial ligand to A_0 in the PsaB subunit of the Chl *a*-binding reaction centre has been engineered both in prokaryotic and eukaryotic PS I RCs (e.g. [37,42–46]). It was shown that substitution of the axial ligand to *ec-A/B3* ($A_{0A/B}$) has the effect of slowing the reduction of the respective electron acceptor, A_{1A} and A_{1B} , from 20–40 ps in the wild-type to ~1.5–2 ns in the mutants [43,45]. The effect of the mutation seems to be relatively independent of the amino acid

engineered to replace the naturally occurring methionine [43,45]. When monitoring the effect of mutations affecting the binding of Chl A_0 , either by substitution of the axial ligand [34,35] or by suppression of H-bonding to the chlorine ring [35,46], at the level of A_1 oxidation, it was shown that, whereas the lifetime of phyloquinone oxidation remained substantially unaltered, a redistribution of the relative contribution of ~20-ns and ~250-ns was observed instead [32,34,35,38,46]. In particular mutants affecting the binding of A_{0A} lead to relative decrease of the amplitude of the 250-ns phase attributed to A_{1A}^- oxidation, whereas mutants affecting A_{0B} lead to a relative decrease of the amplitude associated with A_{1B}^- oxidation [34,35,38,46]. Thus the effect of the mutation is not to “block” charge separation and electron transfer in the affected branch, therefore converting a bi-directional system into a mono-directional one, but rather to “redistribute” the fraction of electrons transferred through each of the active redox chains [34,35,40]. Hence, the naturally occurring amino-acid substitution in *A. marina* PsaB does not, per se, eliminate the possibility of bidirectional electron transfer in this reaction centre. Still, it is somewhat surprising that the amount of B-side electron transfer seems even higher in PS I from this species than it does in Chl *a* containing cyanobacteria.

The significant slowing of PhQ^- oxidation kinetics in *A. marina* compared to Chl *a*-binding reaction centres remains to be explained. Although the rate of PhQ_A^- reoxidation is less than 50% slower in this species, the lifetime of PhQ_B^- reoxidation is larger by a factor of 4–5.

The rate of tunnelling-mediated electron transfer between a donor and an acceptor molecule (k_{ET}) is described by [47,48]:

$$k_{ET} = \frac{4\pi^2}{h} \cdot |H_{DA}|^2 \cdot fc \quad (1)$$

where h is the Planck constant, $|H_{DA}|$ is electronic coupling element, and fc is a function describing the Franck–Condon factors. Considering the coupling of electron transfer with nuclear tunnelling described by a single, mean, oscillator of frequency $\bar{\nu}$, the Franck–Condon factors are described by a Gaussian density function which with respect to the standard Gibbs free energy difference (ΔG^0) has a mean value equal to $-\lambda_t$, the total reorganisation energy, and variance $\sigma^2 = \lambda_t h c \bar{\nu} \cdot \coth \frac{h c \bar{\nu}}{2k_b T}$, where, k_b is the Boltzmann constant and c is the speed of light.

The square of the electron coupling element $|H_{DA}|$ is dependent on the overlap of molecular orbitals, hence the distance between the electron donor and acceptor (r_{DA}). A damping factor (β), that is dependent on the nature of the medium surrounding the reactive moieties, serves a scaling for the length of the potential barrier [47–49], typically approximated by the edge-to-edge distance [47,49]. However, it has been determined that the inter-spin distance between P_{740}^+ and A_1^- in the reaction centre of *A. marina* is substantially the same as in Chl *a*-binding PS I [14]. In the latter case, the inter-spin distances are in close agreement with the structural information [18,20,37]. Hence, this can be taken as an indication that, in a PS I reaction centre containing either Chl *a* or Chl *d*, the binding of A_1 is substantially unaffected. The electron acceptor F_X is co-ordinated at the interface of the PsaA and the PsaB subunits. The cysteine residues known to be involved in forming this iron sulphur cluster, are conserved in the sequence of *psaA* and *psaB* of *A. marina* [19]. Thus, the distance between A_1^- and F_X is very probably the same as in Chl *a*-binding PS I, i.e. ~9 Å. Nonetheless, at present, direct structural information concerning the positioning of F_X in the RC of *A. marina* is not available. Hence, it is not possible to exclude that, since the value of $|H_{DA}|$ decreases exponentially with the length of the tunnelling barrier, which could be approximated by the acceptor-donor edge-to-edge distance, even a small variation in cofactor arrangement could lead to a significant effect on the actual electron transfer rate. Thus, the

slower oxidation kinetics observed in *A. marina* would result from a difference in the binding geometry of the electron transfer cofactors.

Yet, it should also be considered that the difference in oxidation kinetics observed in the Chl *d*-binding complex might originate from changes in the parameters determining the Franck–Condon factor: the free energy difference, ΔG^0 , the reorganisation energy, λ_r , and the mean (phonon) frequency $\bar{\nu}$ coupled to these electron transfer reactions. We consider that the latter is a plausible hypothesis since in Chl *d* based systems there is a significant loss of maximal free energy at disposal for electron transfer reactions (~75–95 meV) compared to Chl *a*-binding systems due to the low energy of the Chl *d* electronic transition. Since the standard redox potential of the electron donor P_{740}^+ was shown to be virtually identical to that of P_{700}^+ [9,12], a drop in free energy difference between the donor acceptor couple on the acceptor side of the reaction centre is then expected.

It is foreseeable that in order to gather conclusive evidence on the directionality in Chl *d*-binding PS I RC of *A. marina* and to gain further insight into the energetic properties of the cofactors, it will be necessary to apply molecular genetic methodologies which have proven crucial for the understanding of electron transfer reactions in Chl *a*-binding reaction centres but which are not yet well developed for this organism.

Acknowledgements

J.B. acknowledges the support of the Biotechnology and Biological Science Research Council (BBSRC). K.R. acknowledges support from DOE grant DE-FG02-08ER15989 and NSF award MCB-1052573. F.R. and B.B. acknowledge support from CNRS and Univ. P. et M. Curie.

References

- [1] H. Miyashita, H. Ikemoto, N. Kurano, K. Adachi, M. Chihara, S. Miyachi, Chlorophyll *d* as a major pigment, *Nature* 383 (1996) 402.
- [2] M. Kühl, M. Chen, P.J. Ralph, U. Schreiber, A.W.D. Larkum, Ecology: a niche for cyanobacteria containing chlorophyll *d*, *Nature* 433 (2005) 820.
- [3] S. Ohashi, H. Miyashita, N. Okada, T. Iemura, T. Watanabe, M. Kobayashi, Unique photosystems in *Acaryochloris marina*, *Photosynth. Res.* 98 (2008) 141–149.
- [4] H. Schiller, H. Senger, H. Miyashita, S. Miyachi, H. Dau, Light-harvesting in *Acaryochloris marina* spectroscopic characterization of a chlorophyll *d*-dominated photosynthetic antenna system, *FEBS Lett.* 410 (1997) 433–436.
- [5] M. Kobayashi, S. Watanabe, T. Gotoh, H. Koizumi, Y. Itoh, M. Akiyama, Y. Shiraiwa, T. Tsuchiya, H. Miyashita, M. Mimuro, T. Yamashita, T. Watanabe, Minor but key chlorophylls in photosystem II, *Photosynth. Res.* 84 (2005) 201–207.
- [6] V.A. Boichenko, V.V. Klimov, H. Miyashita, S. Miyachi, Functional characteristics of chlorophyll *d*-predominating photosynthetic apparatus in intact cells of *Acaryochloris marina*, *Photosynth. Res.* 65 (2000) 269–277.
- [7] Q. Hu, H. Miyashita, I. Iwasaki, N. Kurano, S. Miyachi, M. Iwaki, S. Itoh, A photosystem I reaction center driven by chlorophyll *d* in oxygenic photosynthesis, *Proc. Natl. Acad. Sci. U. S. A.* 95 (1998) 13319–13323.
- [8] S. Itoh, H. Mino, K. Itoh, T. Shigenaga, T. Uzumaki, M. Iwaki, Function of chlorophyll *d* in reaction centers of photosystems I and II of the oxygenic photosynthesis of *Acaryochloris marina*, *Biochemistry* 46 (2007) 12473–12481.
- [9] T. Tomo, Y. Kato, T. Suzuki, S. Akimoto, T. Okubo, T. Noguchi, K. Hasegawa, T. Tsuchiya, K. Tanaka, M. Fukuya, N. Dohmae, T. Watanabe, M. Mimuro, Characterization of highly purified photosystem I complexes from the chlorophyll *d*-dominated cyanobacterium *Acaryochloris marina* MBIC 11017, *J. Biol. Chem.* 283 (2008) 18198–18208.
- [10] S. Kumazaki, K. Abiko, I. Ikegami, M. Iwaki, S. Itoh, Energy equilibration and primary charge separation in chlorophyll *d*-based photosystem I reaction center isolated from *Acaryochloris marina*, *FEBS Lett.* 530 (2002) 153–157.
- [11] M. Schenderlein, M. Çetin, J. Barber, A. Telfer, E. Schlodder, Spectroscopic studies of the chlorophyll *d* containing photosystem I from the cyanobacterium *Acaryochloris marina*, *Biochim. Biophys. Acta* 1777 (2008) 1400–1408.
- [12] B. Baillieu, X. Johnson, G. Finazzi, J. Barber, F. Rappaport, A. Telfer, The thermodynamics and kinetics of electron transfer between cytochrome *b6f* and photosystem I in the chlorophyll *d*-dominated cyanobacterium, *Acaryochloris marina*, *J. Biol. Chem.* 283 (2008) 25218–25226.
- [13] H. Mino, A. Kawamori, D. Aoyama, T. Tomo, M. Iwaki, S. Itoh, Proton ENDOR study of the primary donor P_{740}^+ , a special pair of chlorophyll *d* in photosystem I reaction centre of *Acaryochloris marina*, *Chem. Phys. Lett.* 411 (2005) 262–266.
- [14] S. Santabarbara, M. Chen, A.W. Larkum, M.C.W. Evans, An electron paramagnetic resonance investigation of the electron transfer reactions in the chlorophyll *d* containing photosystem I of *Acaryochloris marina*, *FEBS Lett.* 581 (2007) 1567–1571.
- [15] S. Santabarbara, P. Heathcote, M.C.W. Evans, Modelling of the electron transfer reactions in Photosystem I by electron tunnelling theory: the phylloquinones bound to the PsaA and the PsaB reaction centre subunits of PS I are almost isoenergetic to the iron–sulfur cluster F_X , *Biochim. Biophys. Acta* 1708 (2005) 283–310.
- [16] M.G. Müller, J. Niklas, W. Lubitz, A.R. Holzwarth, Ultrafast transient absorption studies on Photosystem I reaction centers from *Chlamydomonas reinhardtii*. I. A new interpretation of the energy trapping and early electron transfer steps in Photosystem I, *Biophys. J.* 85 (2003) 3899–3922.
- [17] F. Rappaport, B.A. Diner, K.E. Redding, Optical measurements of secondary electron transfer in Photosystem I, in: J. Golbeck (Ed.), *Photosystem I: The Plastocyanin:Ferredoxin Oxidoreductase in Photosynthesis*, Kluwer Academic Publishers, Dordrecht, 2006, pp. 223–244.
- [18] R. Bittl, S. Zech, S.G. Pulsed, EPR spectroscopy of short-lived intermediates in Photosystem I, *Biochim. Biophys. Acta* 1507 (2001) 194–211.
- [19] W.D. Swingle, M. Chen, P.C. Cheung, A.L. Conrad, L.C. Dejesa, J. Hao, B.M. Honchak, L.E. Karbach, A. Kurdoglu, S. Lahiri, S.D. Mastrian, H. Miyashita, L. Page, P. Ramakrishna, S. Satoh, W.M. Sattley, Y. Shimada, H.L. Taylor, T. Tomo, T. Tsuchiya, Z.T. Wang, J. Raymond, M. Mimuro, R.E. Blankenship, J.W. Touchman, Niche adaptation and genome expansion in the chlorophyll *d*-producing cyanobacterium *Acaryochloris marina*, *Proc. Natl. Acad. Sci. U. S. A.* 105 (2008) 2005–2010.
- [20] S. Santabarbara, I. Kuprov, P.J. Hore, A. Casal, P. Heathcote, M.C.W. Evans, Analysis of the spin-polarized electron spin echo of the [$P_{700}^+A_1^-$] radical pair of photosystem I indicates that both reaction centre subunits are competent in electron transfer in cyanobacteria, green algae, and higher plants, *Biochemistry* 45 (2006) 7389–7403.
- [21] M.D. Keller, R.C. Servin, W. Claus, R.R.L. Guillard, Medium for the culture of oceanic ultraphytoplankton, *J. Phycol.* 23 (1987) 633–638.
- [22] D. Beal, F. Rappaport, P. Joliot, A new high-sensitivity 10-ns time-resolution spectrophotometric technique adapted to in vivo analysis of the photosynthetic apparatus, *Rev. Sci. Instrum.* 70 (1999) 202–207.
- [23] S. Santabarbara, K.E. Redding, F. Rappaport, Temperature dependence of the reduction of P_{700}^+ by tightly bound plastocyanin in vivo, *Biochemistry* 48 (2009) 10457–10466.
- [24] S. Santabarbara, K. Reifschneider, A. Jasaitis, F. Gu, G. Agostini, D. Carbonera, F. Rappaport, K.E. Redding, Interquinone electron transfer in Photosystem I as evidenced by altering the hydrogen bond strength to the phylloquinone(s), *J. Phys. Chem. B* 114 (2010) 9300–9312.
- [25] P.D. Bell, Y. Xin, R.E. Blankenship, Purification and characterization of cytochrome c_6 from *Acaryochloris marina*, *Photosynth. Res.* 102 (2009) 43–51.
- [26] A.B. Hope, Electron transfer amongst cytochrome *f*, plastocyanin and Photosystem I: kinetics and mechanism, *Biochim. Biophys. Acta* 1456 (2000) 5–26.
- [27] M. Hippler, F. Drepper, W. Haehnel, J.D. Rochaix, The N-terminal domain of PsaF: precise recognition site for binding and fast electron transfer from cytochrome c_6 and plastocyanin to Photosystem I of *Chlamydomonas reinhardtii*, *Proc. Natl. Acad. Sci. U. S. A.* 95 (1998) 7339–7344.
- [28] J.A. Bautista, F. Rappaport, M. Guergova-Kuras, R.O. Cohen, J.H. Golbeck, J.Y. Wang, D. Beal, B.A. Diner, Biochemical and biophysical characterization of photosystem I from phytoene desaturase and zeta-carotene desaturase deletion mutants of *Synechocystis* sp. PCC 6803: evidence for PsaA- and PsaB-side electron transport in cyanobacteria, *J. Biol. Chem.* 280 (2005) 20030–20041.
- [29] N. Srinivasan, S. Santabarbara, F. Rappaport, D. Carbonera, K.E. Redding, A. van der Est, J.H. Golbeck, Alteration of the H-bond to the A_{1A} phylloquinone in Photosystem I: influence on the kinetics and energetics of electron transfer, *J. Phys. Chem. B* 115 (2011) 1751–1759.
- [30] D.M. Niedzwiedzki, R.E. Blankenship, Singlet and triplet excited state properties of natural chlorophylls and bacteriochlorophylls, *Photosynth. Res.* 106 (2011) 227–238.
- [31] K. Neverov, S. Santabarbara, A.A. Krasnovsky, Phosphorescence study of chlorophyll *d* photophysics. Determination of the energy levels and lifetime of the photo-excited triplet state: evidence of singlet oxygen photosensitization, *Photosynthesis* 108 (2011) 101–106.
- [32] W. Xu, P. Chitnis, A. Valieva, A. van der Est, K. Brettel, M. Guergova-Kuras, J. Pushkar, S. Zech, D. Stehlik, G. Shen, B. Zybailov, J.H. Golbeck, Electron transfer in cyanobacterial photosystem I: II. Determination of forward electron transfer rates of site-directed mutants in a putative electron transfer pathway from A_0 through A_1 to F_X , *J. Biol. Chem.* 278 (2003) 27876–27887.
- [33] K. Brettel, Electron transfer and arrangement of the redox cofactors in Photosystem I, *Biochim. Biophys. Acta Bioenerg.* 1318 (1997) 322–373.
- [34] M. Byrdin, S. Santabarbara, F. Gu, W.V. Fairclough, P. Heathcote, K.E. Redding, F. Rappaport, Assignment of a kinetic component to electron transfer between iron–sulfur clusters F_X and $F_{A/B}$ of Photosystem I, *Biochim. Biophys. Acta* 1757 (2006) 1529–1538.
- [35] S. Santabarbara, A. Jasaitis, M. Byrdin, F. Gu, F. Rappaport, K.E. Redding, Additive effect of mutations affecting the rate of phylloquinone reoxidation and directionality of electron transfer within photosystem I, *Photochem. Photobiol.* 84 (2008) 1381–1387.
- [36] M. Guergova-Kuras, A. Boudreaux, A. Joliot, P. Joliot, K.E. Redding, Evidence for two active branches for electron transfer in Photosystem I, *Proc. Natl. Acad. Sci. U. S. A.* 98 (2001) 4437–4442.
- [37] S. Santabarbara, I. Kuprov, W.V. Fairclough, S. Purton, P.J. Hore, P. Heathcote, M.C.W. Evans, Bidirectional electron transfer in Photosystem I: determination of two distances between P_{700}^+ and A_1^- in spin-correlated radical pairs, *Biochemistry* 44 (2005) 2119–2128.
- [38] S. Santabarbara, L. Galuppini, A.P. Casazza, Bidirectional electron transfer in the reaction centre of photosystem I, *J. Integr. Plant Biol.* 52 (2010) 735–749.

- [39] E. Schlodder, K. Falkenberg, M. Gergeleit, K. Brettel, Temperature dependence of forward and reverse electron transfer from A_1^- , the reduced secondary electron acceptor in photosystem I, *Biochemistry* 37 (1998) 9466–9476.
- [40] S. Santabarbara, I. Kuprov, O. Poluektov, A. Casal, C.A. Russell, S. Purton, M.C.W. Evans, Directionality of electron-transfer reactions in Photosystem I of prokaryotes: universality of the bidirectional electron-transfer model, *J. Phys. Chem. B* 114 (2010) 15158–15171.
- [41] S. Itoh, T. Uzumaki, S. Takaichi, M. Iwaki, S. Kumazaki, K. Itoh, H. Mino, Photosynthesis. Energy from the Sun, in: J.F. Allen, E. Gantt, J.H. Golbeck, B. Osmond (Eds.), 14th International Congress on Photosynthesis, Springer, 2008, pp. 93–96.
- [42] W.V. Fairclough, A. Forsyth, M.C.W. Evans, S.E.J. Rigby, S. Purton, P. Heathcote, Bidirectional electron transfer in photosystem I: electron transfer on the PsaA side is not essential for phototrophic growth in *Chlamydomonas*, *Biochim. Biophys. Acta* 1606 (2003) 43–55.
- [43] V.M. Ramesh, K. Gibasiewicz, S. Lin, S. Bingham, A.N. Webber, Bidirectional electron transfer in Photosystem I: accumulation of A_0^- in A-side or B-side mutants of the axial ligand to chlorophyll A_0 , *Biochemistry* 43 (2003) 1369–1375.
- [44] R.O. Cohen, G. Shen, J.H. Golbeck, W. Xu, P.R. Chitnis, I. Valieva, A. van der Est, Y. Pushkar, D. Stehlik, Evidence for asymmetric electron transfer in cyanobacterial photosystem I: analysis of a methionine-to-leucine mutation of the ligand to the primary electron acceptor A_0 , *Biochemistry* 43 (2004) 4741–4754.
- [45] V.M. Ramesh, K. Gibasiewicz, S. Lin, S.E. Bingham, A.N. Webber, Replacement of the methionine axial ligand to the primary electron acceptor A_0 slows the A_0 – reoxidation dynamics in photosystem I, *Biochim. Biophys. Acta* 1767 (2007) 151–160.
- [46] Y. Li, A. van der Est, M.G. Lucas, V.M. Ramesh, F. Gu, A. Petrenko, S. Lin, A.N. Webber, F. Rappaport, K.E. Redding, Directing electron transfer within Photosystem I by breaking H-bonds in the cofactor branches, *Proc. Natl. Acad. Sci. U. S. A.* 103 (2006) 2144–2149.
- [47] R. Marcus, N. Sutin, Electron transfers in chemistry and biology, *Biochim. Biophys. Acta* 811 (1985) 265–322.
- [48] D. DeVault, *Quantum-Mechanical Tunnelling in Biological Systems*, Cambridge, Cambridge University Press, 1984.
- [49] C.C. Page, C.C. Moser, P.L. Dutton, Mechanism for electron transfer within and between proteins, *Curr. Opin. Chem. Biol.* 7 (2003) 551–556.